Wet-dry hydroclimatic pressure and thermal intensification in contrasting Peruvian basins

Presión hidroclimática húmeda-seca e intensificación térmica en cuencas peruanas contrastantes

Jamil Ramirez[1]*, Luis Velarde[2], Becky Berrocal[2]

1 Universidad Nacional Mayor de San Marcos, Facultad de Ciencias Físicas, E. A. P. de Ingeniería Mecánica de Fluidos. Lima, Perú.
2 Universidad Tecnológica del Perú, Carrera de Ingeniería Civil. Lima, Perú.

SOUTH SUSTAINABILITY

Cite as: Ramirez, J. *et al*. (2026). «Wet-dry hydroclimatic pressure and thermal intensification in contrasting Peruvian basins». *South Sustainability*, 7(2), e174.
DOI: 10.21142/SS-0702-2026-e174

Received: 30/7/2026
Peer reviewed
Accepted: 23/9/2026

© Los autores, 2026. Publicado por la Universidad Científica del Sur (Lima, Perú)

* Corresponding author:
jamil_ramirez.m@hotmail.com

Associate editor:
Alexander Pérez Segovia

ABSTRACT

Peruvian basins span abrupt topographic and climatic gradients, yet sparse, heterogeneous observations hinder consistent basin-scale comparisons of hydroclimatic change. In this study, we developed a multi-product screening framework for nine contrasting basins over the period 1981-2025, using daily precipitation data from CHIRPS, PISCOp v3.0 and ERA5-Land, together with ERA5-Land minimum, mean and maximum temperature data. Four wet indicators (Rx1day, Rx5day, R95pTOT and SDII), four dry indicators (CDD, SPI-3 drought frequency and duration, and annual minimum SPI-12), and four thermal indicators were evaluated using Theil-Sen slopes and Hamed-Rao variance-corrected Mann-Kendall tests, with false-discovery-rate control. Basin-level precipitation intensification data was retained only when at least two products agreed, no product showed a criteria-supported opposite signal, and a minimum effect-size threshold was met. Classification sensitivity was tested across 36 analytical scenarios. The Mayo basin displayed the clearest wet-pressure intensification, with all four wet indicators classified as robust. Mantaro met the criteria for two wet indicators and was wet-dominant under the base cutoff, whereas Grande and Alto Apurímac each retained one robust wet indicator and remained inconclusive. No robust dry indicator was retained in any basin, and no dry-dominant or dual-pressure profile emerged. All basins exhibited ERA5-Land thermal intensification meeting the predefined criteria, with mean-temperature trends of 0.092-0.331°C per decade. Classification was found to be stable in most basins, whereas Mantaro remained strongly threshold-sensitive. The framework distinguishes coherent basin-scale change from product-dependent evidence and supports targeted monitoring and local validation, without implying risk, attribution or vulnerability.

Keywords: *hydroclimatic trends, precipitation extremes, meteorological drought, temperature trends, gridded precipitation products, multi-product analysis*

RESUMEN

Las cuencas peruanas abarcan marcados gradientes climáticos y topográficos, pero la escasez y heterogeneidad de las observaciones dificultan una comparación consistente del cambio hidroclimático a escala de cuenca. Este estudio desarrolló un marco de evaluación basado en múltiples productos para nueve cuencas contrastantes en el periodo 1981-2025, que utilizó precipitación diaria de CHIRPS, PISCOp v3.0 y ERA5-Land, junto con temperaturas mínima, media y máxima de ERA5-Land. Se evaluaron cuatro indicadores húmedos (Rx1day, Rx5day, R95pTOT y SDII), cuatro secos (CDD, frecuencia y duración de sequías SPI-3 y mínimo anual de SPI-12) y cuatro térmicos mediante pendientes de Theil-Sen y pruebas de Mann-Kendall con corrección de varianza de Hamed-Rao y control de la tasa de falsos descubrimientos. La intensificación de la precipitación a escala de cuenca se retuvo únicamente cuando al menos dos productos coincidieron, ningún producto mostró señal opuesta respaldada por los criterios y se superó un umbral mínimo de magnitud; además, la sensibilidad de la clasificación se evaluó mediante 36 escenarios analíticos. Mayo presentó la intensificación de presión húmeda más clara, con sus cuatro indicadores húmedos clasificados como robustos. Mantaro cumplió los criterios en dos indicadores húmedos y fue clasificado como húmedo-dominante bajo el umbral base, mientras que Grande y Alto Apurímac conservaron una señal húmeda robusta cada uno y permanecieron inconclusos. No se retuvo ningún indicador seco robusto en ninguna cuenca, y no se identificaron perfiles seco-dominantes ni de presión dual. Todas las cuencas mostraron intensificación térmica en ERA5-Land que cumplió los criterios predefinidos, con tendencias de temperatura media entre 0.092 y 0.331 °C por década. La clasificación fue estable en la mayoría de las cuencas, mientras que Mantaro permaneció marcadamente sensible al umbral. El marco permite distinguir cambios

coherentes a escala de cuenca de evidencias dependientes del producto y respalda el monitoreo focalizado y la validación local, sin implicar evaluaciones de riesgo, atribución o vulnerabilidad.

Palabras clave: *tendencias hidroclimáticas, extremos de precipitación, sequía meteorológica, tendencias de temperatura, productos de precipitación en rejilla, análisis multiproducto*

1. Introduction

Flood-producing rainfall, persistent dry spells, meteorological drought and warming affect water management, agriculture, ecosystems and infrastructure across multiple hydroclimatic regions (Lozano-Povis *et al*., 2021; Pabon-Caicedo *et al*., 2020; Poveda *et al*., 2020; Spinoni *et al*., 2019). These pressures are particularly consequential where livelihoods and water management are highly dependent upon climatic variability, as is the case in many Peruvian basins. Peru is characterized by sharp hydroclimatic gradients, from arid Pacific catchments to high Andean headwaters, humid Amazonian basins and the Titicaca drainage basin. Observational studies have shown that precipitation and temperature climatologies and trends vary markedly across these settings (Huerta and Lavado-Casimiro, 2021; Imfeld *et al*., 2021), while ENSO and regional circulation modulate precipitation variability and extremes (Jonaitis *et al*., 2021; Villalobos-Puma *et al*., 2022). A single national tendency cannot, therefore, be employed to represent the hydroclimatic pressures experienced by individual basins. Comparable basin-scale screening is needed to identify where signals are coherent, where they remain uncertain, and where local verification should receive greater attention.

Gridded climate products provide spatially complete and reproducible records for poorly gauged basins. CHIRPS combines satellite infrared estimates with station observations (Funk *et al*., 2015). The Peru-specific gridded precipitation dataset used in this study was PISCOp v3.0, the latest version of the PISCO precipitation product available for the study period, hereafter abbreviated as PISCO for consistency with the figures and tables (Aybar *et al*., 2020; Gutiérrez and Lavado-Casimiro, 2025). ERA5-Land provides a land-focused reanalysis for terrestrial applications (Muñoz-Sabater *et al*., 2021). Other Peru-focused products, including RAIN4PE and PISCOp_h, illustrate recent advances in daily and hourly precipitation coverage (Fernández-Palomino *et al*., 2022; Huerta *et al*., 2022). These products are not interchangeable, because differences in spatial resolution, station incorporation, satellite retrievals, bias correction and reanalysis physics affect precipitation estimates, particularly in the case of steep terrain and low-rainfall climates (Rajulapati *et al*., 2020). A multi-product approach, therefore, characterizes uncertainty while preserving disagreement, rather than averaging it away (Zhou *et al*., 2020).

Annual precipitation data does not identify short-duration extremes, wet-day intensity or dry-spell persistence, for which distinct indicators are required (Dunn *et al*., 2020). SPI results are dependent upon distributional assumptions, reference periods and stationarity choices (Cammalleri *et al*., 2022; Laimighofer and Laaha, 2022). The framework of this study, therefore, separated wet, dry and thermal domains, applied statistical and effect-size criteria, and evaluated classification sensitivity. Agricultural and urban footprints provide context but do not measure exposure, vulnerability or risk (Heikkinen, 2021). For this study, we developed a reproducible hydroclimatic screening framework for nine contrasting Peruvian basins over the period 1981-2025. It asked: (i) which wet, dry and thermal signals occurred; (ii) which precipitation signals agreed across products; and (iii) which wet-dry profiles remained stable under alternative analytical settings? The study's contribution constitutes a compact method for comparing ungauged or poorly gauged basins, without overstating what can be established using gridded historical data.

2. Materials and methods

2.1. Study area and datasets

Our analysis was applied to nine official hydrographic units: Piura, Chancay-Lambayeque, Rímac, Grande, Mantaro, Mayo, Pachitea, Azángaro and Alto Apurímac. Their boundaries were obtained from the national hydrographic framework of Peru's National Water Authority (ANA), defined in accordance with the Pfafstetter classification system; no basin was redelineated for this study. The nine units were selected in order to provide broad geographical coverage across northern, central and southern Peru and across Pacific, Andean-Amazonian, Amazonian and Titicaca drainage settings. The selection was intended to represent contrasting hydroclimatic environments, rather than a probabilistic or exhaustive sample of Peruvian basins. Topographic background and basin elevation statistics were derived from FABDEM V1-2, a global bare-earth digital elevation model with a spatial resolution of 1 arc second, approximately 30 m at the equator (Hawker *et al*., 2022; Neal and Hawker, 2023). Their locations, boundaries and elevation patterns are shown in Figure 1.

The basin areas ranged from 3504 km² to 34,683 km², and the mean elevations ranged from 453 m to 4367 m. The elevation ranges and territorial fractions are summarized in Table 1. The agricultural fractions were calculated using agricultural-area polygons from the *Atlas de la Superficie Agrícola del Perú* (*Ministerio de Desarrollo Agrario y Riego*, 2021), and the urban fractions were obtained from urban-area polygons produced by the Peruvian National Institute for Statistics and Informatics (INEI). These layers represent only area-based territorial footprints, and should not be interpreted as population exposure or vulnerability.

 DOI: 10.21142/SS-0702-2026-e174

Daily CHIRPS precipitation (Funk *et al.*, 2015) and ERA5-Land daily aggregated precipitation and air temperature data (Muñoz-Sabater *et al.*, 2021) were accessed and processed from Google Earth Engine using the UCSB-CHG/CHIRPS/DAILY and ECMWF/ERA5_LAND/DAILY_AGGR collections, respectively. Daily basin-average values were extracted over the ANA basin polygons using a spatial mean reducer. ERA5-Land supplied daily precipitation and minimum, mean and maximum air temperature. PISCOp v3.0 daily precipitation (Gutiérrez and Lavado-Casimiro, 2025) was downloaded from Figshare and processed separately in R, where the gridded data were spatially clipped to the same ANA basin polygons and converted to daily basin-average series. The three precipitation products were retained as separate product estimates throughout indicator calculation and signal assessment and were not assumed to be statistically or observationally independent. Potential evapotranspiration was not included in the final analysis.

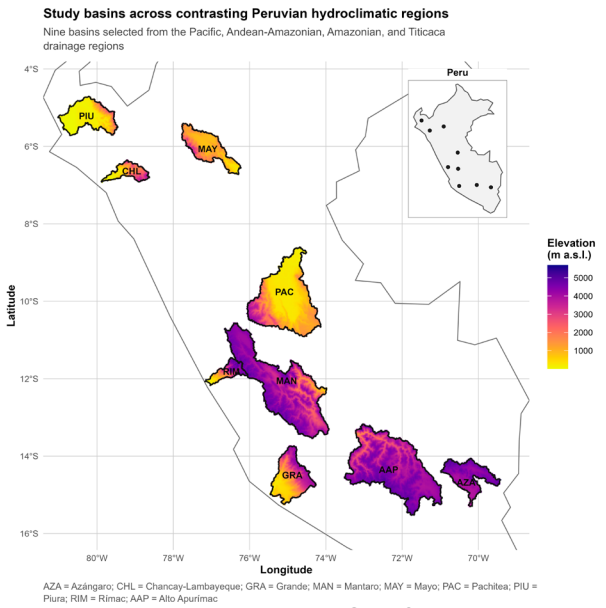


Figure 1. Location, topography and identifiers of the nine study basins

2.2. Preprocessing and indicators

The precipitation and temperature series were processed separately. Dates, basin identifiers, product names and units were harmonized, duplicated basin-date records were checked, negative precipitation values were rejected, and records in which Tmin exceeded Tmax were treated as invalid. Annual precipitation and temperature indicators were retained when at least 90% of the expected daily observations within the same calendar year were valid. Trend estimation required at least 30 valid annual values. The precipitation products were not merged or averaged before trend estimation and cross-product signal assessment.

Wet pressure was represented by annual maximum one-day precipitation (Rx1day), annual maximum five-day precipitation (Rx5day), precipitation from wet days above the basin, product-specific 95th percentile for the period 1981-2010 (R95pTOT) and the simple daily intensity index (SDII). Together with consecutive dry days (CDD), these metrics are consistent with widely used indices for characterizing precipitation extremes (Dunn *et al.*, 2020). Dry pressure was represented by CDD, the annual number of months with SPI-3 below −1, the maximum within-year duration of this condition, and the annual minimum SPI-12. Because SPI estimates can vary according to distributional choices, record length, accumulation scale and reference period, the results were interpreted as dataset- and configuration-dependent evidence (Laimighofer and Laaha, 2022; Wang *et al.*, 2021). The base dry-day threshold was 1 mm per day, while 0.5 mm per day was evaluated in the sensitivity analysis. The indicator definitions, units, effect-size thresholds and analytical roles are summarized in Table 2. A precipitation signal was considered operationally robust when at least two of the three products each met the trend-direction, adjusted-significance and effect-size criteria, while no product showed a criteria-supported signal in the opposite direction. This criterion represents cross-product consistency, rather than independent observational

Table 1. Basin characteristics and territorial footprints

Basin ID	Basin	Area (km2)	Mean elevation (m)	Elevation range (m)	Agricultural area (km2)	Agricultural fraction (%)	Urban area (km2)	Urban fraction (%)
AZA	Azángaro	8803.7	4367	1930	939.9	10.68	22.35	0.254
CHL	Chancay-Lambayeque	4042.8	1626	4112	1253.3	31	28.04	0.694
GRA	Grande	11058.5	2124	4636	493.9	4.47	22.22	0.201
MAN	Mantaro	34569.1	3881	5221	5653	16.35	442.12	1.279
MAY	Mayo	9768.7	1288	3805	4223.3	43.23	114.6	1.173
PAC	Pachitea	28669	1040	4982	5635.4	19.66	26.05	0.091
PIU	Piura	10936.4	453	3671	3355.5	30.68	171.44	1.568
RIM	Rímac	3504.1	2946	5578	125.6	3.58	460.71	13.148
AAP	Alto Apurímac	34683.3	4064	5233	2845.5	8.2	87.4	0.252

Note. Mean elevation and elevation range were derived from the digital elevation model. Agricultural area was obtained from the *Atlas de la Superficie Agrícola del Perú* (*Ministerio de Desarrollo Agrario y Riego*, 2021), and urban area from INEI polygons. The fractions represent the percentage of each basin occupied by these territorial footprints and do not indicate population exposure or vulnerability.

validation, because CHIRPS, PISCO and ERA5-Land are not fully independent datasets.

The R95pTOT threshold was calculated separately for each basin and precipitation product using wet days with precipitation of at least 1 mm during the period 1981-2010. Monthly precipitation totals used for SPI calculation were retained only when at least 90% of the expected daily observations in the corresponding month were available; otherwise, the monthly value was treated as missing and was not imputed. Zero monthly precipitation totals were retained and handled within the SPI calculation through the estimated probability of zero precipitation. They were not replaced or imputed. SPI-3 and SPI-12 were calculated over the period 1981-2025 using a Gamma distribution fitted through unbiased probability-weighted moments. Annual SPI-derived indicators were retained only when at least 90% of the corresponding monthly SPI values were available within the same calendar year, equivalent to at least 11 of 12 months. Meteorological drought months were defined by SPI-3 < −1. SPI-3 drought duration was calculated as the longest uninterrupted drought sequence within each calendar year; sequences crossing December-January were therefore split at the calendar year boundary. Thermal conditions were described using annual means of daily Tmin, Tmean, Tmax and the diurnal temperature range. Tmin, Tmean and Tmax were not treated as three independent pressure votes; instead, they jointly defined a thermal modifier, separating widespread warming from the wet-dry classification. ERA5-Land thermal intensification was considered as meeting the predefined criteria when Tmin and Tmax increased, Tmean also increased, and at least one of Tmin or Tmax met both the adjusted-significance and effect-size criteria. This classification was based exclusively on ERA5-Land and therefore does not constitute multi-product confirmation.

Table 2. Indicator definitions, interpretation and base effect-size thresholds

Domain	Indicator	Definition	Unit	Criterion for intensification	Role in the analysis
Wet	Annual precipitation	Total precipitation accumulated during the year	mm per year	Increase of at least 5% per decade	Descriptive context
Wet	Rx1day	Highest daily precipitation recorded within each year	mm	Increase of at least 5% per decade	Wet-pressure score
Wet	Rx5day	Highest precipitation accumulated over five consecutive days within each year	mm	Increase of at least 5% per decade	Wet-pressure score
Wet	R95pTOT	Annual precipitation accumulated on days exceeding the basin- and product-specific 95th percentile for 1981-2010	mm per year	Increase of at least 5% per decade	Wet-pressure score
Wet	SDII	Mean precipitation intensity on days with at least 1 mm of precipitation	mm per wet day	Increase of at least 3% per decade	Wet-pressure score
Dry	CDD	Highest number of consecutive days with precipitation below 1 mm within each year	days	Increase of at least 2 days per decade	Dry-pressure score
Dry	SPI-3 drought frequency	Number of months within each year in which SPI-3 was below −1	months per year	Increase of at least 0.5 months per year over a decade	Dry-pressure score
Dry	SPI-3 drought duration	Longest uninterrupted sequence of months within each year in which SPI-3 was below −1	months	Increase of at least 0.25 months per decade	Dry-pressure score
Dry	Annual minimum SPI-12	Lowest monthly SPI-12 value recorded within each year	SPI units	Decrease of at least 0.1 SPI units per decade	Dry-pressure score
Thermal	Tmin	Annual mean of daily minimum air temperature	°C	Increase of at least 0.1°C per decade	Thermal modifier
Thermal	Tmean	Annual mean air temperature	°C	Positive trend supporting the thermal classification	Thermal modifier
Thermal	Tmax	Annual mean of daily maximum air temperature	°C	Increase of at least 0.1°C per decade	Thermal modifier
Thermal	DTR	Annual mean difference between daily maximum and minimum air temperature	°C	No directional criterion assigned	Thermal context

Note. Base effect-size thresholds refer to changes per decade. Dry days were defined using a threshold of 1 mm per day in the base analysis and 0.5 mm per day in the sensitivity analysis. Tmin, Tmean and Tmax were evaluated jointly as a thermal modifier and were not counted as separate wet-dry pressure indicators.

DOI: 10.21142/SS-0702-2026-e174

2.3. Trends, product agreement and profile classification

For each basin, product and indicator, we quantified monotonic change per decade using the Theil-Sen slope and evaluated statistical significance with the Mann-Kendall test. For indicators evaluated through relative effect sizes, percentage change per decade was calculated by dividing the decadal Theil-Sen slope by the absolute median of the corresponding annual series. These non-parametric procedures are widely used for monotonic trend assessment; however, their results can be sensitive to temporal granularity and the treatment of serial autocorrelation (Collaud Coen *et al.*, 2020). Mann-Kendall significance was evaluated using the Hamed-Rao variance-corrected procedure to account for temporal autocorrelation in the annual series (Hamed and Rao, 1998). Theil-Sen slopes were retained as the estimator of trend magnitude.

Subsequently, the Benjamini-Hochberg procedure was applied to the autocorrelation-corrected p-values, in order to control the false discovery rate across the nine basins separately for each product-indicator combination (Benjamini and Hochberg, 1995). Additionally, in the CDD sensitivity analysis, the adjustment was performed separately for each dry-day threshold. The base adjusted significance level was 0.10. As a complementary measure of temporal change, median indicator values for the periods 1981-2002 and 2004-2025 were compared using 2000 bootstrap resamples and percentile-based 95% confidence intervals. The year 2003 was excluded from this comparison only, in order to obtain two equal 22-year periods and remained included in the complete 1981-2025 period trend analysis. Bootstrap comparisons were treated as supporting descriptive evidence and did not determine product-level signals or wet-dry profile classifications.

At the product level, intensification required a trend in the expected direction, an adjusted p-value not exceeding the selected significance level, and an effect size meeting the corresponding threshold. The effect-size thresholds were defined as operational screening criteria, rather than as universal physical boundaries. Their purpose was to prevent statistically supported but very small changes from determining the basin-level classification. The base thresholds for wet indicators were increases of 5% per decade for Rx1day, Rx5day and R95pTOT, and 3% per decade for SDII. For dry indicators, the thresholds were increases of 2 days per decade for CDD, 0.5 months per decade in the annual number of SPI-3 drought months, and 0.25 months per decade for SPI-3 duration, together with a decrease of at least 0.1 SPI units per decade for the annual minimum SPI-12. Because these thresholds are screening choices, rather than physically unique limits, their influence was explicitly evaluated in the sensitivity analysis by multiplying all base effect-size thresholds by 0.75, 1.00 and 1.25.

A precipitation signal was classified as robust intensification when at least two of the three products met the product-level criteria and no product showed a criteria-supported change in the opposite direction. The term «robust» is used here as an operational descriptor of consistency across products and should not be interpreted as evidence from three statistically or observationally independent datasets. Wet (W) and dry (D) scores were calculated as the proportions of the four indicators in each domain classified as robustly intensifying. Using a base cutoff of 0.50, basins were classified as wet-dominant when $W \geq 0.50$ and $D < 0.50$, dry-dominant when $D \geq 0.50$ and $W < 0.50$, dual-pressure when both scores were ≥ 0.50, and inconclusive when both scores were < 0.50. ERA5-Land thermal intensification was considered as meeting the predefined criteria when Tmin, Tmean and Tmax all exhibited positive trends and at least one of Tmin or Tmax met both the adjusted-significance and effect-size criteria. This ERA5-Land-based classification was treated as a modifier of the wet-dry profile, rather than as an additional pressure axis.

2.4. Sensitivity and territorial interpretation

Classification sensitivity was evaluated using 36 scenarios combining two CDD thresholds (0.5 and 1 mm per day), three effect-size multipliers (0.75, 1.00 and 1.25), two adjusted significance levels (0.05 and 0.10), and three W-D profile cutoffs (0.40, 0.50 and 0.60). The effect-size multipliers were included specifically to test the dependence of the basin classifications on the operational magnitude thresholds used in the screening framework. Classification stability was quantified as the proportion of scenarios assigned to the modal profile. Agricultural and urban fractions were used solely to support the territorial interpretation of the hydroclimatic profiles and to identify questions requiring more detailed monitoring or local assessment. They were not combined with hydroclimatic signals to construct a composite index, risk score, vulnerability measure or priority ranking. All analyses were conducted in R 4.6.0. The principal packages used included dplyr 1.2.1 and tidyr 1.3.2 for data manipulation, SPEI 1.8.1 for SPI calculation, modifiedmk 1.6 for autocorrelation-corrected Mann-Kendall tests, sf 1.1.2, terra 1.9.34 and exactextractr 0.10.1 for spatial processing, and ggplot2 4.0.3 for visualization. A complete record of package versions is provided with the reproducibility materials.

3. Results

3.1. Hydroclimatic signals and product agreement

Daily data completeness met the threshold required to retain all annual precipitation and temperature series in the 45-year analysis. Precipitation signals varied substantially across basins and products, whereas temperature trends consistently indicated warming. Robust wet intensification was strongest in the Mayo and

Mantaro basins, with one additional robust wet indicator in both Grande and Alto Apurímac. No robust dry indicator was retained under the autocorrelation-corrected analysis (Figure 2). Mayo displayed robust intensification in all four wet indicators: Rx1day, Rx5day, R95pTOT and SDII. Median effect sizes across the three product-specific estimates were +8.9%, +5.6%, +20.2% and +4.7% per decade, respectively. Mantaro showed robust intensification in Rx1day and R95pTOT, with median effect sizes of +5.2% and +12.1% per decade, respectively. Grande retained robust intensification only in Rx1day (+12.6% per decade), whereas Alto Apurímac retained only R95pTOT (+12.0% per decade). Azángaro, Chancay-Lambayeque, Piura, Pachitea and Rímac displayed no robust wet indicators under the base criteria. In Rímac, however, Rx1day, R95pTOT and SDII showed conflicting criteria-supported signals among precipitation products, representing the clearest indication of cross-product disagreement. No dry indicator met the cross-product robustness criterion in any basin, after accounting for temporal autocorrelation. Directional changes were detected more frequently at the individual-product level, but these did not meet the combined adjusted-significance, effect-size and cross-product criteria required for classification as robust basin-level signals. All nine basins met the predefined ERA5-Land thermal-intensification criteria. Tmean increased from 0.092°C per decade in Piura to 0.331°C per decade in Alto Apurímac. Tmin trends ranged from 0.080°C to 0.259°C per decade, whereas Tmax trends ranged from 0.105°C to 0.390°C per decade. Alto Apurímac exhibited the highest warming rates, while Piura showed the lowest rates for all three temperature metrics. Overall, the cross-product rule substantially reduced the number of precipitation signals retained at the basin level and distinguished consistent intensification from isolated or contradictory product-level trends. The resulting counts of robust wet and dry signals, the indicators retained in each basin, and the principal case of cross-product disagreement are summarized in Table 3. Complete numerical trend estimates, Theil-Sen slopes, Mann-Kendall statistics, raw and adjusted p-values, effect-size evaluations and product-level signal classifications are provided in Supplementary Tables S1 and S3. Median changes and bootstrap confidence intervals for the 1981-2002 and 2004-2025 periods are reported in Supplementary Table S2.

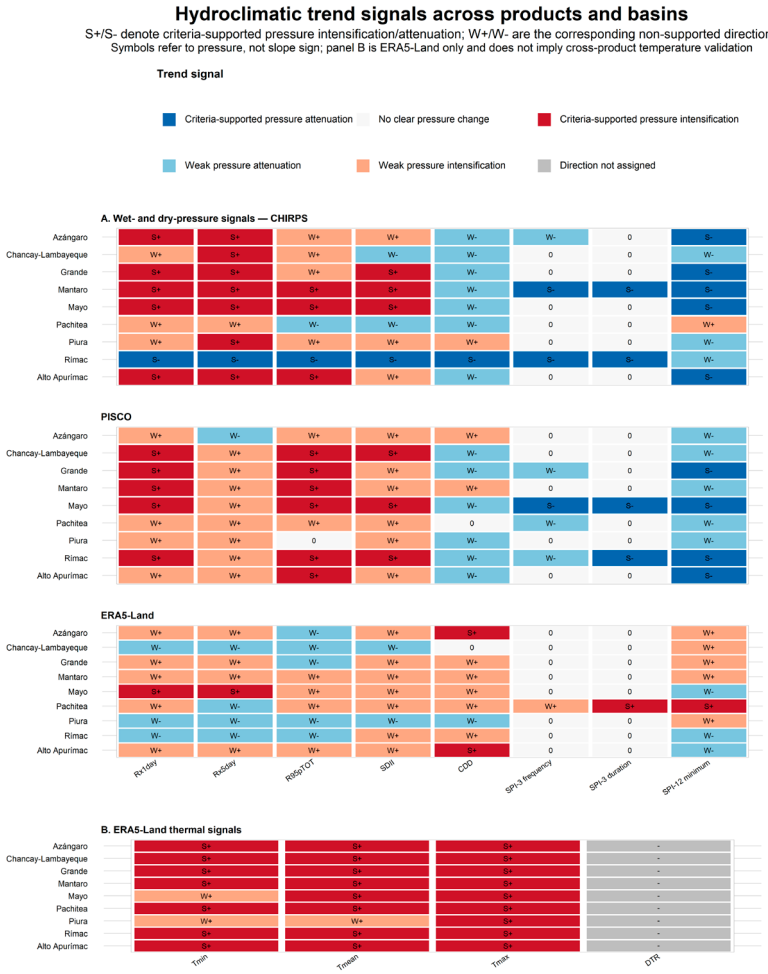


Figure 2. Hydroclimatic trend signals across products and basins. (A) Wet- and dry-pressure signals from CHIRPS, PISCO and ERA5-Land. (B) ERA5-Land thermal signals. S+/S− indicate criteria-supported pressure intensification/attenuation; W+/W− indicate corresponding non-supported directions. Zero denotes no clear change, and a dash indicates that no direction was assigned.

DOI: 10.21142/SS-0702-2026-e174

Table 3. Basin-level cross-product agreement and robust wet and dry indicators

Basin	Robust wet signals (n/4)	Robust dry signals (n/4)	Robust wet indicators	Robust dry indicators	Indicators with conflicting product signals
Azángaro	0	0	—	—	—
Chancay-Lambayeque	0	0	—	—	—
Grande	1	0	Rx1day	—	—
Mantaro	2	0	Rx1day; R95pTOT	—	—
Mayo	4	0	Rx1day; Rx5day; R95pTOT; SDII	—	—
Pachitea	0	0	—	—	—
Piura	0	0	—	—	—
Rímac	0	0	—	—	Rx1day; R95pTOT; SDII
Alto Apurímac	1	0	R95pTOT	—	—

Note. Each basin was evaluated using four wet and four dry indicators. Robust signals met the cross-product agreement, adjusted-significance and effect-size criteria. Conflicting signals indicate opposing criteria-supported product-level results for the same indicator. An em dash indicates that no indicator met the corresponding condition.

3.2. Wet-dry profiles and thermal modification

Using the base cutoff, Mayo had W = 1.00 and D = 0, while Mantaro had W = 0.50 and D = 0. These two basins were therefore classified as wet-dominant. Grande and Alto Apurímac each had W = 0.25 and D = 0, whereas Azángaro, Chancay-Lambayeque, Pachitea, Piura and Rímac had W = D = 0. The remaining seven basins were classified as inconclusive, and none met the dry-dominant or dual-pressure criteria (Figure 3). Mantaro lay exactly at the base wet-score cutoff (W = 0.50), meaning that its wet-dominant classification depended on retaining a cutoff of 0.50 or lower; nevertheless, its two supported wet indicators showed positive continuous effect magnitudes, with median changes of +5.2% per decade for Rx1day and +12.1% per decade for R95pTOT. Mayo was clearly separated from this classification boundary with W = 1.00, whereas Grande and Alto Apurímac remained below it with W = 0.25. Under the study's analysis, no basin retained a robust dry indicator. These results illustrate why the categorical profiles should be interpreted together with the underlying effect magnitudes, W-D scores and sensitivity results. Territorial footprints differed markedly across different basins. The agricultural fractions were highest in Mayo (43.23%), Chancay-Lambayeque (31.00%) and Piura (30.68%). Rímac had the largest urban fraction (13.15%), substantially exceeding that of the other basins despite its inconclusive wet-dry profile. These contrasts may serve to guide more detailed local assessments, but they cannot be employed to establish impacts or priorities without additional information related to population, infrastructure, water management and vulnerability. Exact W and D scores, temperature trends, classification stability and territorial fractions are summarized in Table 4.

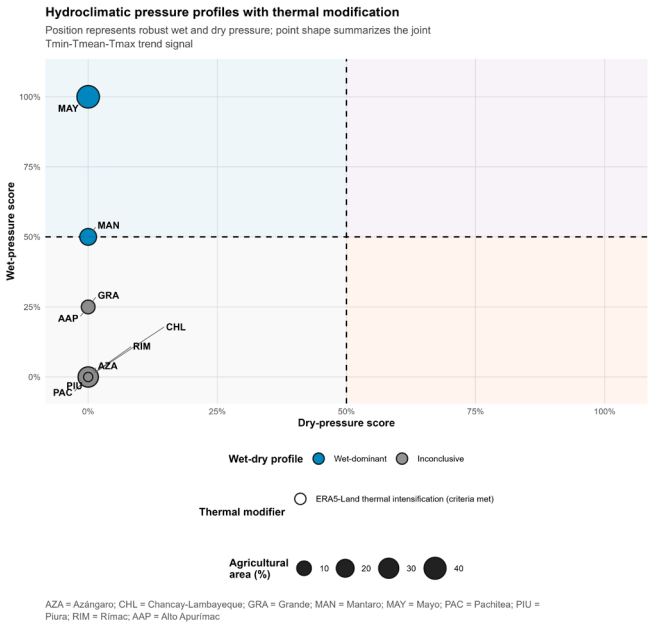


Figure 3. Wet-dry pressure space for the nine basins. All basins share an ERA5-Land thermal-intensification modifier meeting the predefined criteria.

Table 4. Final wet-dry profiles, thermal trends, sensitivity stability and territorial footprints

Basin	W	D	Base profile	Tmin / Tmean / Tmax (°C/decade)	Modal sensitivity profile	Stability	Agricultural area (%)	Urban area (%)
Azángaro	0.00	0.00	Inconclusive	0.196 / 0.283 / 0.333	Inconclusive	1.000	10.68	0.254
Chancay-Lambayeque	0.00	0.00	Inconclusive	0.158 / 0.171 / 0.175	Inconclusive	1.000	31.00	0.694
Grande	0.25	0.00	Inconclusive	0.161 / 0.205 / 0.211	Inconclusive	1.000	4.47	0.201
Mantaro	0.50	0.00	Wet-dominant	0.197 / 0.213 / 0.215	Inconclusive	0.556	16.35	1.279
Mayo	1.00	0.00	Wet-dominant	0.093 / 0.116 / 0.146	Wet-dominant	1.000	43.23	1.173
Pachitea	0.00	0.00	Inconclusive	0.177 / 0.245 / 0.309	Inconclusive	1.000	19.66	0.091
Piura	0.00	0.00	Inconclusive	0.080 / 0.092 / 0.105	Inconclusive	1.000	30.68	1.568
Rímac	0.00	0.00	Inconclusive	0.222 / 0.207 / 0.193	Inconclusive	1.000	3.58	13.148
Alto Apurímac	0.25	0.00	Inconclusive	0.259 / 0.331 / 0.390	Inconclusive	0.889	8.20	0.252

Note. W and D are the proportions of wet and dry indicators, respectively, classified as robustly intensifying under the base criteria. Stability is the proportion of the 36 sensitivity scenarios assigned to the modal profile. All basins met the predefined ERA5-Land thermal-intensification criteria; therefore, the common thermal modifier is not repeated as a separate column. Agricultural and urban percentages represent descriptive territorial footprints only.

3.3. Sensitivity and classification stability

The Azángaro, Chancay-Lambayeque, Grande, Mayo, Pachitea, Piura and Rímac basins retained the same classification across all 36 sensitivity scenarios. Alto Apurímac was classified as inconclusive in 88.9% of the scenarios. Mantaro displayed the greatest sensitivity: it was inconclusive in 55.6% of the scenarios despite being wet-dominant under the base settings. No sensitivity scenario produced a dry-dominant or dual-pressure profile. Classification changes were restricted to the boundary between wet-dominant and inconclusive in Mantaro and, less frequently, Alto Apurímac. Mantaro was wet-dominant under the base settings but inconclusive in 55.6% of the 36 scenarios, making the inconclusive profile its modal sensitivity outcome. Grande was inconclusive in all tested scenarios after the autocorrelation correction. The absence of robust dry-pressure signals was also maintained across the tested methodological settings (Figure 4). The complete set of classifications obtained under the 36 sensitivity scenarios and the corresponding basin-level stability summaries are provided in Supplementary Tables S5 and S6.

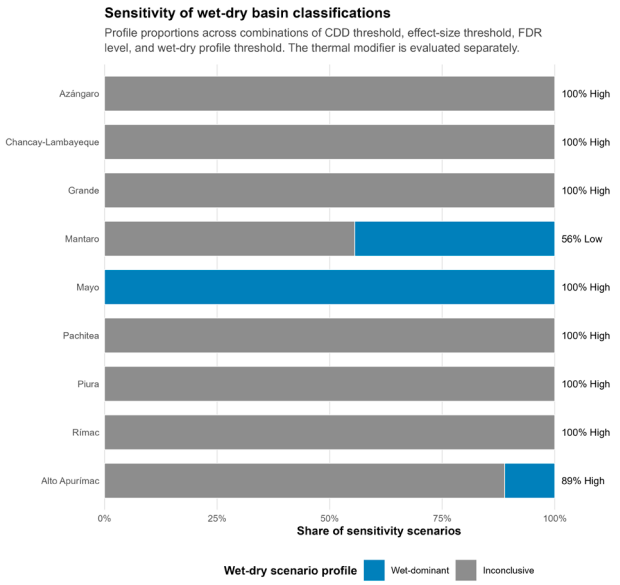


Figure 4. Proportion of the 36 sensitivity scenarios assigned to each observed wet-dry profile. Only profiles that occurred are displayed.

4. Discussion

4.1. Contrasting basin trajectories and widespread warming

The results of our study show contrasting precipitation trajectories under a shared warming signal. Mayo intensified across all four wet indicators, whereas Mantaro met the cross-product criteria for two. Grande and Alto Apurímac retained one wet indicator each and remained inconclusive. Because Mantaro lies exactly at the classification cutoff, its wet-dominant profile should be interpreted conditionally. The marked differences across basins are consistent with previous evidence that precipitation trends and extremes are spatially heterogeneous across southern Peru and the Peruvian Altiplano (Huerta and Lavado-Casimiro, 2021; Imfeld *et al.*, 2021). Studies of summertime extremes on the western Andean slopes also emphasize the role of regional atmospheric circulation (Villalobos-Puma *et al.*, 2022), while high-resolution projections suggest that increases in heavy precipitation can coexist with stronger drought pressure in glacierized Peruvian basins (Potter *et al.*, 2023). These studies differ from the present analysis in terms of domain, period and data, meaning that the comparison is qualitative rather than a direct validation.

DOI: 10.21142/SS-0702-2026-e174

Limited evidence of dry-pressure intensification does not imply the absence of drought events or water stress. Recent studies have documented significant drought episodes in the Peruvian Amazon (Martínez-Castro *et al*., 2025) and ENSO-related agricultural drought in the Mantaro Valley (Arana Ruedas and Moggiano, 2023), but event occurrence and sectoral drought impacts are not equivalent to a monotonic trend in basin-scale meteorological indicators. The indicators used in this study do not represent hydrological drought, reservoir storage, water demand or operational scarcity. Wet extremes and persistent dry anomalies may also evolve independently or concurrently, as suggested by high-resolution modeling in the Peruvian Andes (Potter *et al*., 2023). The absence of dry indicators that satisfy the cross-product criteria therefore reinforces the need for evidence from several indicators, before assigning a basin-wide dry-dominant profile. Thermal intensification was the only result shared by all the basins, although its magnitude varied substantially. Alto Apurímac showed higher warming rates than Piura for Tmin, Tmean and Tmax. This widespread warming is consistent with evidence of increasing temperatures across the Andes, although magnitudes vary according to elevation, season, dataset and period (Imfeld *et al*., 2021; Pabon-Caicedo *et al*., 2020). Rising temperatures may affect evaporative demand, crop water requirements, soil moisture and snow-related processes; modeling in glacierized Peruvian basins further suggests that warming-driven evapotranspiration can intensify drought pressure, even where precipitation increases (Potter *et al*., 2023). However, potential evapotranspiration and these associated responses were not quantified in this study, and should therefore be regarded as plausible mechanisms requiring further evaluation, rather than as additional measured pressure components.

4.2. Product dependence and territorial implications

Because precipitation estimates remain uncertain over complex terrain, cross-product agreement was required. Evaluations of global precipitation datasets indicate that their representation of extremes can differ markedly (Rajulapati *et al*., 2020), and multi-product approaches provide a transparent means of describing this uncertainty (Zhou *et al*., 2020). In the Peruvian context, the development and evaluation of PISCO and RAIN4PE highlight the challenges posed by sparse gauges, steep topography and strong climatic gradients (Aybar *et al*., 2020; Fernández-Palomino *et al*., 2022). The availability of higher-frequency products such as PISCOp_h expands potential applications but does not by itself remove product dependence from trend assessment (Huerta *et al*., 2022). In Rímac, three wet indicators indicated conflicting criteria-supported signals among products, illustrating this problem in a steep basin extending from the arid coast to high-elevation headwaters. A diagnosis based on a single product would have appeared more conclusive, but would have been less defensible.

Territorial fractions provide context for the interpreting of the hydroclimatic profiles. The Mayo basin combined the strongest wet-pressure profile with the largest agricultural fraction, supporting the need for more detailed evaluation of drainage, erosion, crop management and accessibility during intense rainfall. This is consistent with broader evidence that Andean agriculture is sensitive to climatic change and extremes (Lozano-Povis *et al*., 2021). The Chancay-Lambayeque and Piura basins had large agricultural fractions, but also displayed inconclusive wet-dry profiles, indicating that local station assessment and product evaluation would be necessary, before firmer conclusions could be drawn. Rímac combined the largest urban fraction with substantial disagreement among precipitation products, supporting finer-scale rainfall and drainage analyses, rather than a basin-wide risk classification. These territorial interpretations should be considered conditional, because vulnerability is dependent upon livelihood, institutions, power relations and adaptive capacity, in addition to climatic signals (Heikkinen, 2021). Territorial interpretations should be considered qualitative, because area fractions do not measure spatial overlap with people, infrastructure or adaptive capacity. Vulnerability also reflects place-specific social and institutional processes (Heikkinen, 2021); therefore, the study framework supports local investigation, rather than national adaptation rankings.

4.3. Limitations and transferability

In this study, we did not validate the identified trends against discharge records or dense station networks, and nor did we evaluate hydrological response. Basin-average series may conceal elevation-dependent patterns, rain shadows, headwater-lowland contrasts and localized extremes. In addition, the agricultural and urban layers represent static territorial footprints and do not capture land-use change during the study period. Population exposure, infrastructure, livelihoods, social vulnerability and management capacity remained outside the analytical scope of the study.

The historical trends do not establish anthropogenic attribution and should not be interpreted as climate projections. SPI results are dependent on the selected precipitation dataset, accumulation scale, probability distribution, reference period and the assumption that the underlying precipitation regime is sufficiently stationary (Cammalleri *et al*., 2022; Laimighofer and Laaha, 2022; Wang *et al*., 2021). The categorical profiles are dependent on operational thresholds that simplify continuous hydroclimatic evidence and should not be interpreted as universal physical boundaries. The sensitivity analysis explicitly evaluates this dependence across alternative effect-size, significance, CDD and profile thresholds, but cannot represent every defensible methodological choice. The most transferable elements of the framework are the

separation of wet, dry and thermal domains, the explicit cross-product agreement rule, the use of minimum effect-size criteria, and the evaluation of classification sensitivity. Applications in other regions would require locally appropriate datasets, quality-control procedures, reference periods and thresholds. The Peruvian precipitation products and territorial layers are context-specific, but the analytical workflow could be adapted to other data-scarce basins. Cross-product agreement should be interpreted as consistency among distinct gridded precipitation products, rather than as fully independent observational validation. CHIRPS, PISCO and ERA5-Land differ in their construction and data sources, but they cannot be assumed to provide fully independent evidence. Consequently, agreement among them increases confidence in the consistency of the detected signal across products, but does not replace validation against an independent dense rain-gauge network.

Thermal trends were evaluated using ERA5-Land alone. Consequently, the thermal modifier indicates compliance with the predefined ERA5-Land-based trend. Significance and effect-size criteria should not be interpreted as multi-product confirmation or independent temperature validation.

5. Conclusions

Across nine contrasting Peruvian basins during the period 1981-2025, robust wet-pressure intensification was strongest in the Mayo and Mantaro basins. Mayo exhibited robust change in all four wet indicators, whereas Mantaro met the criteria for two, and Grande and Alto Apurímac retained one wet indicator each. Mayo and Mantaro were classified as wet-dominant under the base rules, while the remaining seven basins were classified as inconclusive. No robust dry indicator was retained in any basin, and no basin was classified as dry-dominant or subject to dual wet-dry pressure. In contrast, all nine basins met the predefined ERA5-Land thermal-intensification criteria, with Tmean trends ranging from 0.092°C to 0.331°C per decade. The requirement for agreement among precipitation products prevented isolated or contradictory signals from determining the basin-level profiles. Most of the classifications were stable across the 36 sensitivity scenarios, while Mantaro remained close to the wet-profile boundary. In the case of Mantaro, the modal sensitivity classification differed from the base result. Consequently, categorical labels near the cutoff should be interpreted together with the underlying continuous effect sizes, W and D scores, and their sensitivity distributions. The proposed framework provides a transparent and reproducible first screening of hydroclimatic pressure in poorly gauged basins. While its results can support the selection of basins and questions for more detailed monitoring, validation and local assessment, they should not be interpreted as risk rankings or as evidence of impacts, vulnerability, climate attribution or future change. Engineering and adaptation decisions require local observations and explicit analyses of hydrological response, exposure, infrastructure, management and social vulnerability.

Supplementary material

The Supplementary Results section contains eight worksheets: S1, complete trend estimates; S2, median changes and bootstrap confidence intervals between the two historical periods; S3, product-level signal classifications; S4, cross-product agreement results; S5, the 36 profile-sensitivity scenarios; S6, basin-level classification stability; S7, ERA5-Land thermal trends; and S8, thermal-modifier results.

Authors' contributions

Jamil Ramirez: Conceptualization, methodology, software, formal analysis, investigation, data curation, visualization, and writing (original draft).

Luis Velarde: Validation, data curation, and writing (revision and editing).

Becky Berrocal: Supervision, project administration, writing (revision and editing).

All three authors reviewed and approved the final version of the manuscript.

Research funding

The research was self-funded by the authors and received no external funding.

Conflicts of interest

The authors declare no conflicts of interest.

Data and code availability

PISCO (PISCOp v3.0) daily precipitation data were downloaded from Figshare and are publicly available at https://doi.org/10.6084/m9.figshare.32411886. CHIRPS daily precipitation (UCSB-CHG/CHIRPS/DAILY) and ERA5-Land daily aggregated precipitation and temperature (ECMWF/ERA5_LAND/DAILY_AGGR) data were accessed and processed through the Google Earth Engine Data Catalog. The basin boundaries were obtained from the official hydrographic framework of Peru's National Water Authority (ANA). Urban-area and agricultural-area polygons were obtained from INEI and MIDAGRI, respectively. The processed basin-level series, indicator outputs, supplementary analytical results, R scripts and Google Earth Engine scripts are available from the corresponding author upon reasonable request.

Artificial Intelligence use statement

During the preparation of this study, the authors used ChatGPT and Codex (OpenAI) to assist with manuscript editing, code generation, code debugging and workflow

organization. All analytical procedures, scripts, results and interpretations were critically reviewed, verified and, where necessary, modified by the authors. The authors take full responsibility for the accuracy, reproducibility and integrity of the study and the final manuscript.

Bibliographic references

Arana Ruedas, D. P. R., and Moggiano, N. (2023). «ENSO influence on agricultural drought identified by SPEI assessment in the Peruvian tropical Andes, Mantaro Valley». *Manglar*, 20(2), pp. 157-167. Available at: https://revistas.untumbes.edu.pe/index.php/manglar/en/article/view/379

Aybar, C., Fernández, C., Huerta, A., Lavado, W., Vega, F., and Felipe-Obando, O. (2020). «Construction of a high-resolution gridded rainfall dataset for Peru from 1981 to the present day». *Hydrological Sciences Journal*, 65(5), pp. 770-785. Available at: https://www.tandfonline.com/doi/full/10.1080/02626667.2019.1649411

Benjamini, Y., and Hochberg, Y. (1995). «Controlling the false discovery rate: a practical and powerful approach to multiple testing». *Journal of the Royal Statistical Society: Series B (Methodological)*, 57(1), pp. 289-300. Available at: https://rss.onlinelibrary.wiley.com/doi/10.1111/j.2517-6161.1995.tb02031.x

Cammalleri, C., Spinoni, J., Barbosa, P., Toreti, A., and Vogt, J. V. (2022). «The effects of non-stationarity on SPI for operational drought monitoring in Europe». *International Journal of Climatology*, 42(6), pp. 3418-3430. Available at: https://rmets.onlinelibrary.wiley.com/doi/10.1002/joc.7424

Collaud Coen, M., Andrews, E., Bigi, A., Martucci, G., Romanens, G., Vogt, F. P. A., and Vuilleumier, L. (2020). «Effects of the prewhitening method, the time granularity, and the time segmentation on the Mann-Kendall trend detection and the associated Sen's slope». *Atmospheric Measurement Techniques*, 13(12), pp. 6945-6964. Available at: https://amt.copernicus.org/articles/13/6945/2020/

Dunn, R. J. H., Alexander, L. V., Donat, M. G., Zhang, X., Bador, M., Herold, N., Lippmann, T., Allan, R., Aguilar, E., Barry, A. A., Brunet, M., Caesar, J., Chagnaud, G., Cheng, V. Y. S., Cinco, T., Durre, I., de Guzman, R., Htay, T. M., Wan Ibadullah, W. M., Bin Ibrahim, M. K. I., Khoshkam, M., Kruger, A., Kubota, H., Leng, T. W., Lim, G., Li-Sha, L., Marengo, J., Mbatha, S., McGree, S., Menne, M. J., Skansi, M. de los M., Ngwenya, S., Nkrumah, F., Oonariya, C., Pabon-Caicedo, J. D., Panthou, G., Pham, C., Rahimzadeh, F., Ramos, A., Salgado, E., Salinger, J., Sane, Y., Sopaheluwakan, A., Srivastava, A., Sun, Y., Timbal, B., Trachow, N., Trewin, B., van der Schrier, G., Vazquez-Aguirre, J., Vasquez, R., Villarroel, C., Vincent, L., Vischel, T., Vose, R., and Yussof, M. N. (2020). «Development of an updated global land in situ-based data set of temperature and precipitation extremes: HadEX3». *Journal of Geophysical Research: Atmospheres*, 125(16), e2019JD032263. Available at: https://agupubs.onlinelibrary.wiley.com/doi/full/10.1029/2019JD032263

Fernández-Palomino, C. A., Hattermann, F. F., Krysanova, V., Lobanova, A., Vega-Jacome, F., Lavado, W., Santini, W., Aybar, C., and Bronstert, A. (2022). «A novel high-resolution gridded precipitation dataset for Peruvian and Ecuadorian watersheds: development and hydrological evaluation». *Journal of Hydrometeorology*, 23(3), pp. 309-336. Available at: https://journals.ametsoc.org/view/journals/hydr/23/3/JHM-D-20-0285.1.xml

Funk, C., Peterson, P., Landsfeld, M., Pedreros, D., Verdin, J., Shukla, S., Husak, G., Rowland, J., Harrison, L., Hoell, A., and Michaelsen, J. (2015). «The Climate Hazards Infrared Precipitation with Stations—a new environmental record for monitoring extremes». *Scientific Data*, 2(1), 150066. Available at: https://www.nature.com/articles/sdata201566

Gutiérrez, L., and Lavado-Casimiro, W. (2025). «High-resolution grids of rainfall for Peru - PISCOp v3.0 dataset». Figshare. Available at: https://figshare.com/articles/dataset/High-resolution_grids_of_rainfall_for_Peru_-_PISCOp_v3_0_dataset/32411886

Hamed, K. H., and Rao, A. R. (1998). «A modified Mann-Kendall trend test for autocorrelated data». *Journal of Hydrology*, 204(1-4), pp. 182-196. Available at: https://www.sciencedirect.com/science/article/abs/pii/S002216949700125X

Hawker, L., Uhe, P., Paulo, L., Sosa, J., Savage, J., Sampson, C., and Neal, J. (2022). «A 30 m global map of elevation with forests and buildings removed». *Environmental Research Letters*, 17(2), 024016. Available at: https://iopscience.iop.org/article/10.1088/1748-9326/ac4d4f

Heikkinen, A. M. (2021). «Climate change, power, and vulnerabilities in the Peruvian Highlands». *Regional Environmental Change*, 21(3), 82. Available at: https://link.springer.com/article/10.1007/s10113-021-01825-8

Huerta, A., and Lavado-Casimiro, W. (2021). «Trends and variability of precipitation extremes in the Peruvian Altiplano (1971-2013)». *International Journal of Climatology*, 41(1), pp. 513-528. Available at: https://rmets.onlinelibrary.wiley.com/doi/10.1002/joc.6635

Huerta, A., Lavado-Casimiro, W., and Felipe-Obando, O. (2022). «High-resolution gridded hourly precipitation dataset for Peru (PISCOp_h)». *Data in Brief*, 45, 108570. Available at: https://www.sciencedirect.com/science/article/pii/S2352340922007776

Imfeld, N., Sedlmeier, K., Gubler, S., Correa Marrou, K., Davila, C. P., Huerta, A., Lavado-Casimiro, W., Rohrer, M., Scherrer, S. C., and Schwierz, C. (2021). «A combined view on precipitation and temperature climatology and trends in the southern Andes of Peru». *International Journal of Climatology*, 41(1), pp. 679-698. Available at: https://rmets.onlinelibrary.wiley.com/doi/10.1002/joc.6645

Jonaitis, J. A., Perry, L. B., Soule, P. T., Thaxton, C., Andrade-Flores, M. F., Vargas, T. I., and Ticona, L. (2021). «Spatiotemporal patterns of ENSO-precipitation relationships in the tropical Andes of southern Peru and Bolivia». *International Journal of Climatology*, 41(8), pp. 4061-4076. Available at: https://rmets.onlinelibrary.wiley.com/doi/abs/10.1002/joc.7058

Laimighofer, J., and Laaha, G. (2022). «How standard are standardized drought indices? Uncertainty components for the SPI & SPEI case». *Journal of Hydrology*, 613, 128385. Available at: https://www.sciencedirect.com/science/article/pii/S0022169422009544

Lozano-Povis, A., Álvarez-Montalvan, C. E., and Moggiano, N. (2021). «Climate change in the Andes and its impact on agriculture: a systematic review». *Scientia Agropecuaria*, 12(1), pp. 101-108. https://revistas.unitru.edu.pe/index.php/scientiaagrop/es/article/view/3341

Martínez-Castro, D., Takahashi, K., Espinoza, J.-C., Vichot-Llano, A., Andrade, M. O., and Silva, F. Y. (2025). «Extreme droughts in the Peruvian Amazon region (2000-2024)». *Water*, 17(12), 1744. Available at: https://www.mdpi.com/2073-4441/17/12/1744

Ministerio de Desarrollo Agrario y Riego (2021). *Atlas de la superficie agrícola del Perú*. Lima: *Ministerio de Desarrollo Agrario y Riego*. Available at: https://repositorio.midagri.gob.pe/handle/20.500.13036/1197

Muñoz-Sabater, J., Dutra, E., Agusti-Panareda, A., Albergel, C., Arduini, G., Balsamo, G., Boussetta, S., Choulga, M., Harrigan, S., Hersbach, H., Martens, B., Miralles, D. G., Piles, M., Rodríguez-Fernández, N. J., Zsoter, E., Buontempo, C., and Thepaut, J.-N. (2021). «ERA5-Land: a state-of-the-art global reanalysis dataset for land applications». *Earth System Science Data*, 13(9), pp. 4349-4383. Available at: https://essd.copernicus.org/articles/13/4349/2021/

Neal, J., and Hawker, L. (2023). *FABDEM V1-2*. Dataset. Bristol: University of Bristol Research Data Repository. doi: 10.5523/bris.s5hqmjcdj8yo2ibzi9b4ew3sn.

Pabon-Caicedo, J. D., Arias, P. A., Carril, A. F., Espinoza, J. C., Fita, L., Goubanova, K., Lavado-Casimiro, W., Masiokas, M., Solman, S., and Villalba, R. (2020). «Observed and projected hydroclimate changes in the Andes». *Frontiers in Earth Science*, 8, 61. Available at: https://www.frontiersin.org/journals/earth-science/articles/10.3389/feart.2020.00061/full

Potter, E. R., Fyffe, C. L., Orr, A., Quincey, D. J., Ross, A. N., Rangecroft, S., Medina, K., Burns, H. K., Llacza, A., Jacome, G., Hellstrom, R. A., Castro, J., Cochachin, A., Montoya, N., Loarte, E., and Pellicciotti, F. (2023). «A future of extreme precipitation and droughts in the Peruvian Andes». *npj Climate and Atmospheric Science*, 6(1), 96. Available at: https://www.nature.com/articles/s41612-023-00409-z

Poveda, G., Espinoza, J. C., Zuluaga, M. D., Solman, S. A., Garreaud, R., and van Oevelen, P. J. (2020). «High impact weather events in the Andes». *Frontiers in Earth Science*, 8, 162. Available at: https://www.frontiersin.org/journals/earth-science/articles/10.3389/feart.2020.00162/full

Rajulapati, C. R., Papalexiou, S. M., Clark, M. P., Razavi, S., Tang, G., and Pomeroy, J. W. (2020). «Assessment of extremes in global precipitation products: how reliable are they?». *Journal of Hydrometeorology*, 21(12), pp. 2855-2873. Available at: https://ntrs.nasa.gov/api/citations/20230000902/downloads/Rajulapti_2020_PDFA.pdf

Spinoni, J., Barbosa, P., De Jager, A., McCormick, N., Naumann, G., Vogt, J. V., Magni, D., Masante, D., and Mazzeschi, M. (2019). «A new global database of meteorological drought events from 1951 to 2016». *Journal of Hydrology. Regional Studies*, 22, 100593. Available at: https://www.sciencedirect.com/science/article/pii/S2214581818303136

Villalobos-Puma, E., Flores-Rojas, J. L., Martínez-Castro, D., Morales, A., Lavado-Casimiro, W., Mosquera-Vásquez, K., and Silva, Y. (2022). «Summertime precipitation extremes and the influence of atmospheric flows on the western slopes of the southern Andes of Peru». *International Journal of Climatology*, 42(16), pp. 9909-9930. Available at: https://rmets.onlinelibrary.wiley.com/doi/10.1002/joc.7871

Wang, W., Wang, J., and Romanowicz, R. J. (2021). «Uncertainty in SPI calculation and its impact on drought assessment in different climate regions over China». *Journal of Hydrometeorology*, 22(6), pp. 1369-1383. Available at: https://journals.ametsoc.org/view/journals/hydr/22/6/JHM-D-20-0256.1.xml

Zhou, X., Polcher, J., Yang, T., and Huang, C.-S. (2020). «A new uncertainty estimation approach with multiple datasets and implementation for various precipitation products». *Hydrology and Earth System Sciences*, 24(4), pp. 2061-2081. Available at: https://hess.copernicus.org/articles/24/2061/2020/